Neovascular AMD

2

Eric H. Souied and Francesca Amoroso

Abbreviations

BNV	Branching type 1 neovascular network
BVN	Branching vascular network
CNV	Choroidal neovascularization
CRA	Chorio-retinal anastomosis
ICGA	ICG angiography
NV	Neovascularization
OCRA	Occult choroidal retinal anastomosis
OCTA	OCT-Angiography
PCV	Polypoidal choroidal vasculopathy
PDT	Photodynamic therapy
PED	Pigment epithelium detachment
PRN	"Pro-Re-Nata"
RAP	Retinal angiomatous proliferation
RPE	Retinal pigment epithelium
SRD	Serous retinal detachment
SRF	Subretinal fluid
VEGF	Vascular endothelial growth factor
v-PED	Vascularized PED

Introduction

Neovascular AMD is defined by the presence of choroidal and/or intraretinal neovascularization with associated exudation, bleeding, and disciform scar (Ferris III et al. 1984). Choroidal neovascularization (CNV) is characterized by an abnormal growth of newly formed vessels within the macular area.

Different types of neovascular growth pattern have been described: pigment epithelial or type 1 choroidal neovascularization, preretinal pigment epithelial or type 2 choroidal neovascularization, and retinal angiomatous proliferation or type 3 neovascularization (NV) (Grossniklaus and Gass 1998; Yannuzzi et al. 2001; Freund et al. 2010; Cohen et al. 2007a, b; Jung et al. 2014).

Donald M. Gass described the histopathologic and fluorescein angiographic characteristics of CNV, defining as type 1 CNV the neovascularization proliferating under the retinal pigment epithelium (RPE) with less distinct margins and less actively proliferating than other types of neovascularization, with a poorly defined or "occult" CNV pattern on fluorescein angiography (FA) (Grossniklaus and Gass 1998).

Gass also described type 2 CNV as the neovascularization characterized by the active proliferation of the new vessels beneath the neurosensory retina, showing a well-defined or "classic" pattern of fluorescence on fluorescein angiography.

A third anatomic subtype of neovascularization in AMD has been described; type 3 neovascularization is characterized by the presence of an intraretinal neovascularization in conjunction with a compensatory proliferative response that is featured by perfusing arterioles, draining venules, and the eventual formation of anastomoses between the intraretinal proliferation and sub-RPE neovascularization.

The main feature of type 3 NV is the active proliferation within neurosensory retina; however, a concomitant choroidal component has been described (Yannuzzi et al. 2001; Freund et al. 2008).

Another form of neovascularization is polypoidal choroidal vasculopathy (PCV), which is considered a variant of type 1 neovascularization because it is located in the subpigment epithelial space. A branching type 1 neovascular network (BNV), similar to type 1 CNV with terminal aneurysmal changes (polyps), has been associated with PCV (Yannuzzi et al. 1990; Laude et al. 2010; Yannuzzi 1982). The frequency of neovascular subtypes in neovascular AMD in white patients is approximately 40% type 1, 9% type 2, 34% type 3, and 17% mixed (Jung et al. 2014; Cohen et al. 2007a).

E. H. Souied (✉) · F. Amoroso
Department of Ophthalmology, Centre Hospitalier Intercommunal de Créteil, Université de Paris Est Créteil, Créteil, France
e-mail: eric.souied@chicreteil.fr

I. K. Kim (ed.), *Macular Disorders*, Retina Atlas, https://doi.org/10.1007/978-981-15-3001-2_2

Classification and Diagnosis of Neovascular AMD: The Multimodal Imaging

Type 1 Neovascularization

Type 1 neovascularization originates from the choroid and extends under the RPE, with subsequent detachments of the RPE and overlying retina.

On fundus examination, type 1 CNV presents with moderate exudative signs.

The subretinal fluid (SRF) responsible for the functional syndrome is usually mild; retinal hemorrhages are rarely observed, although occult CNV can be complicated by extensive hematoma. Deep exudates are more common, whereas cystoid macular edema, unusual in the early form, is later formed. Finally, the precursors of AMD are present (drusen and abnormalities of the RPE).

On fluorescein angiography, type 1 CNV is poorly defined and inhomogeneous with early staining of the lesion, including hyperfluorescent pinpoints. On late phases of the angiographic sequence, the lesion increases in size, and leakage is observed. The precise limits of the neovascular lesion cannot be easily determined. The typical aspect of this CNV is the early hyperfluorescence on ICG angiography (ICGA), with the appearance of a "plaque" in late stages.

The SD-OCT shows increased central macular thickness (associated with RPE detachment), subretinal fluid, edema, and/or intraretinal cyst (Fig. 2.1). The SD-OCT examination shows, depending on the stage of evolution, the presence of an RPE elevation or pigment epithelium detachment (PED) (98% of cases). The elevation of the RPE is initially moderate, separated from the moderate reflectivity of Bruch's membrane by a hyporeflective space. The PED can, however, become very extensive. The presence of an occult CNV may be suspected due to an irregular, fragmented, or thickened appearance of the RPE. All exudative signs may be present: SRF, hyper-reflective points (Coscas et al. 2013), pre-epithelial exudation (Ores et al. 2014), and cystoid cells within the neurosensory retina.

On OCT-Angiography (OCTA), the type 1 neovascular lesion was compared to a "blossoming tree" or a "seafan pattern" to describe the typical aspect of the lesion: a central feeder vessel with neovessels radiating from the central trunk in both directions and on one side of the lesion. A more advanced lesion, called mature lesion, can harbor a tangled or a dead tree pattern (Fig. 2.2) (Kuehlewein et al. 2015).

Vascularized PED

Type 1 CNV, commonly described as a vascularized PED (v-PED), is a sign of hidden or "occult" neovascularization (Mrejen et al. 2013).

It generally appears as a well-circumscribed yellow-orange RPE bulge, showing late staining on fluorescein angiography. The SD-OCT typically shows heterogeneous sub-RPE signal and subretinal fluid (Fig. 2.3).

Vascularized PEDs may present a mixture of serous, drusenoid, and vascularized components. Fluorescein angiography reveals hyperfluorescent "pin-points" in late phases, whilst ICGA shows the early appearance of neovascular network with a late "plaque." SD-OCT reveals the elevation of the RPE, subretinal fluid, and exudation. The sub-RPE material may be heterogeneous, with serous, drusenoid, and vascular components.

Furthermore, vascularized PED variants have been described as:

- Multilayered PED (Rahimy et al. 2014)
- The "onion sign" (Pang et al. 2015)
- Retinal pigment epithelium tears/apertures (Querques et al. 2016)
- Wrinkled-PED (Lam et al. 2017)
- Quiescent type 1 (Querques et al. 2013c)

Type 2 Choroidal Neovascularization

Type 2 CNV, is called subretinal CNV or "well-defined CNV" because of its appearance on FA. Although it is less frequent than type 1 CNV, it is also known as classic CNV because it was the first pattern to be described on FA. Type 2 CNV originates from the choroidal circulation, penetrates through the pigmented epithelium, and extends into the subretinal space leading to bleeding and exudative features such as SRD and/or edema. This type of CNV actively proliferates below the neurosensory retina.

On fundus and color pictures, classic CNVs are not directly discernible in early stages, but result in discrete retinal thickening with a greyish-white retinal aspect. Exudative signs, the SRF, retinal or subretinal hemorrhages, lipied exudates, and intraretinal cystoid edema, are barely present (Grossniklaus and Gass 1998). PED is rare in pure visible pre-epithelial neovessels. The IR pictures reveal the presence of a multilayered structure. This structure appears as a complex with a dark central core surrounded by a whitish reflective ring, giving a halo-like shape (Semoun et al. 2009).

Fluorescein angiography typically shows an early staining of the lesion that appears as a *bicycle wheel* or an *umbrella pattern*. The classic CNV lesion is hyperfluorescent, commonly contrasting with a surrounding hypofluorescent ring. On late phase of the FA sequence, an intense leakage is observed associated with dye pooling in subretinal space in late stages. In some cases, the hyperfluorescence of the dye may decrease on late phase, corresponding to the "wash-out effect."

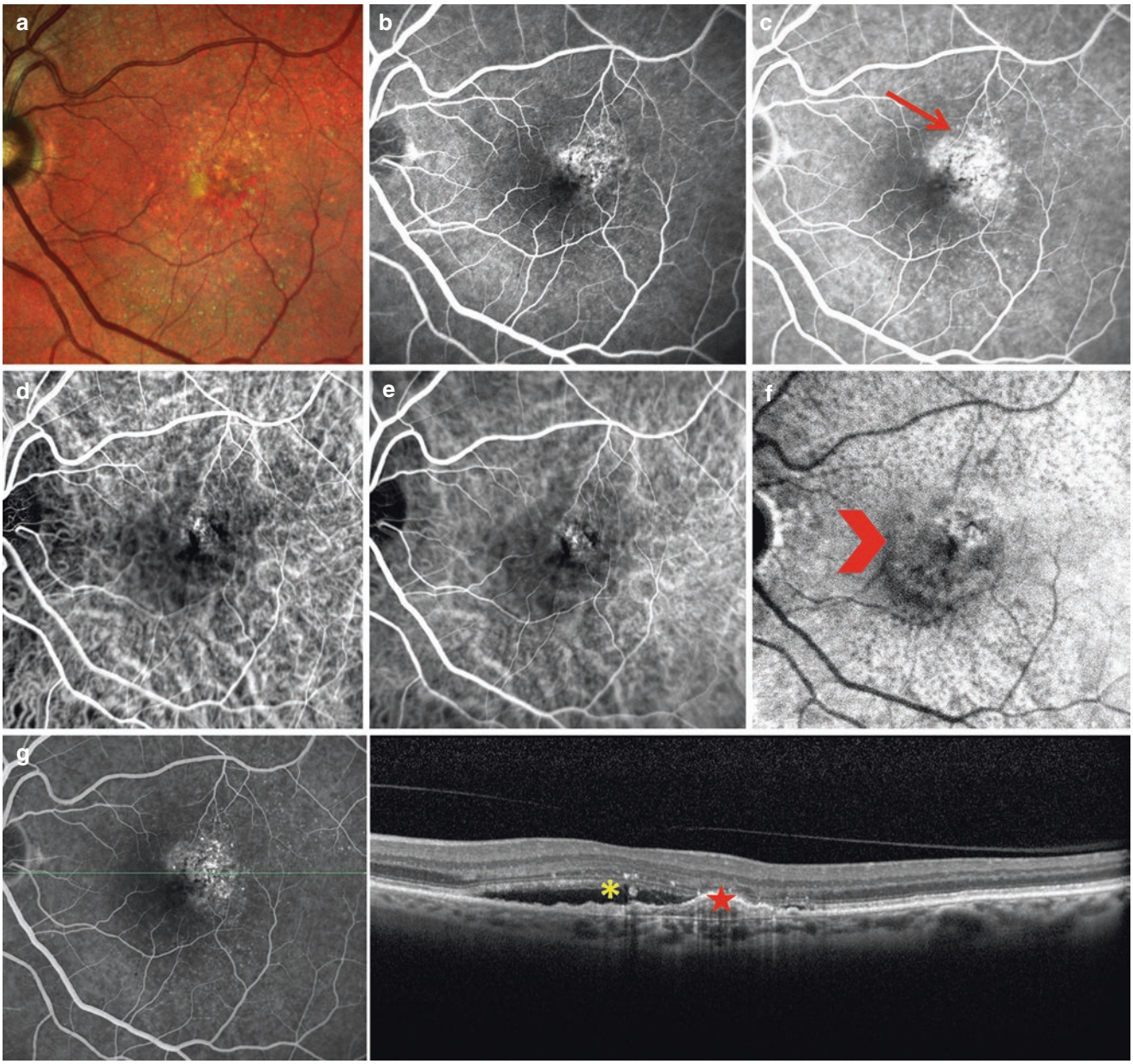

Fig. 2.1 Multimodal imaging of a patient with type 1 CNV. (**a**) Multicolor imaging shows the presence of a PED temporal to the fovea, reticular pseudodrusen at the posterior pole and the absence of exudates or hemorrhages; hyperfluorescent pinpoints in the early stages (**b**) persisting in late phases (arrow) (**c**) on fluorescein angiography; ICGA shows hypercyanescence of subretinal neovascularization in the early stages (**d**), persistence in the intermediate stages (**e**) and hypercyanescent "plaque" in late phases (arrowhead) (**f**); (**g**) SD-OCT showing the presence of a PED corresponding to the CNV (star), accompanied by subretinal fluid (asterisk)

Indocyanine green angiography reveals the early filling and the washout of the neovascular membrane in late stages (Grossniklaus and Gass 1998; Cohen et al. 2007a; Gelisken et al. 1998).

The OCT shows the typical hyperreflective fusiform lesion above the RPE, with or without visible effraction signs.

On SD-OCT, a serous retinal detachment can be seen, most often present on the edges of the fusiform lesion and the *grey hyperreflective subretinal exudation* (Ores et al. 2014), sign of neovascular lesion activity, as well as intraretinal cysts and serous detachment of neuroepithelium (Fig. 2.4).

Type 2 neovascularizations represent only 10% of neovascular AMD cases, but type 2 CNV is the most common lesion type in pathological myopia, angioid streaks, and multifocal choroiditis.

Several patterns of type 2 neovascularization have been described on OCTA, with a constant high flow appearance present both in the outer retinal segmentation and in the

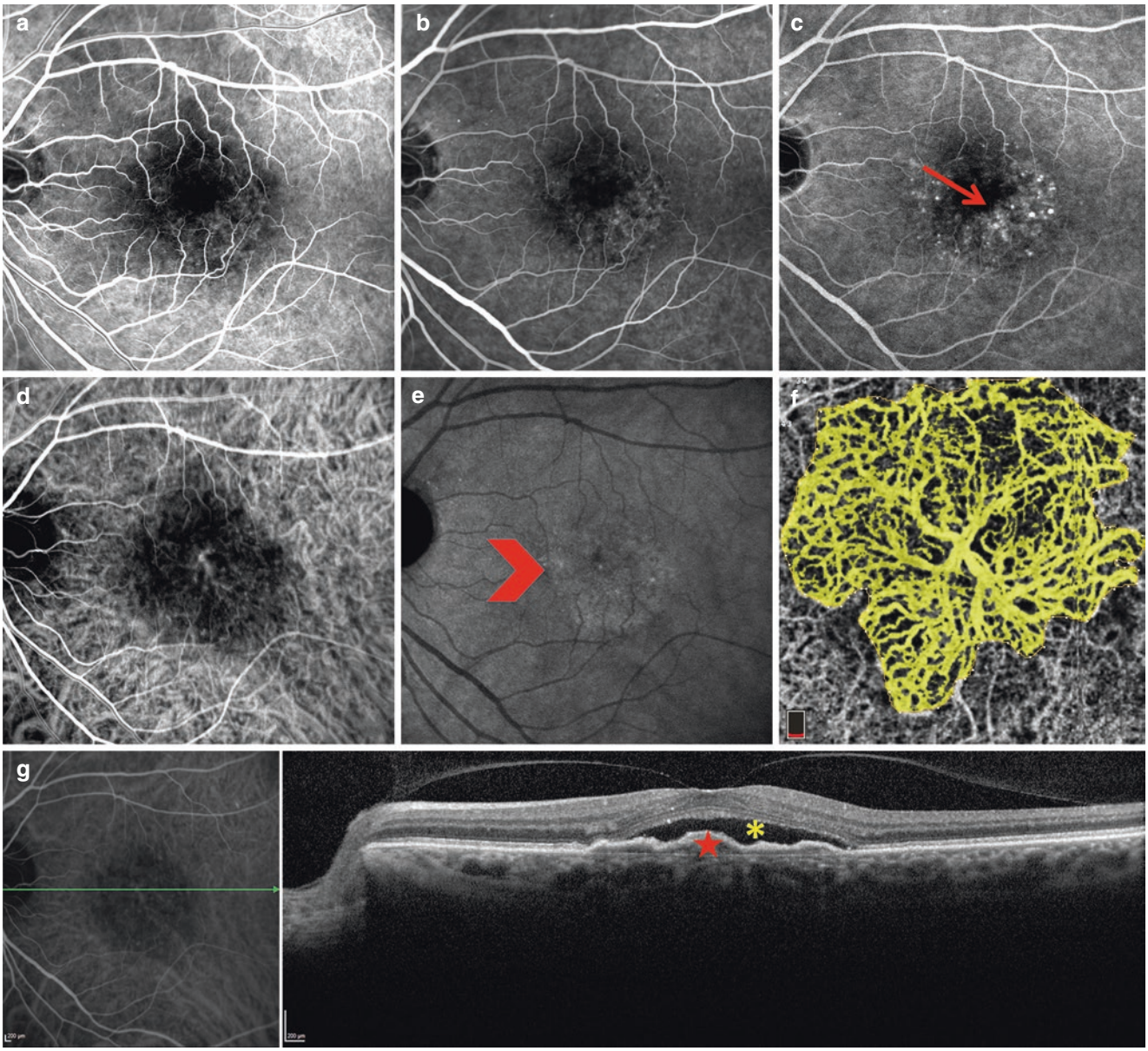

Fig. 2.2 Multimodal imaging of a patient with type 1 CNV: (**a**) hyperfluorescent pinpoints appearing in early phases (**b**) persisting in late stages (arrow) (**c**) on fluorescein angiography; ICG shows the hypercyanescence of subretinal neovessels in early stages (**d**) and the appearance of the "plaque" in late phases (arrowhead) (**e**); (**f**) OCTA 3 × 3 scan highlights a large neovascular membrane, characterized by a central trunk with small, high-flowing vessels branching in all directions. The image is almost overlapping with the ICGA; (**g**) SD-OCT shows the PED (star), accompanied by suburetinal fluid (asterisk)

choriocapillaris segmentation. OCTA showed a 100% sensitivity in the detection of type 2 CNVs (El Ameen et al. 2015).

Based on the different morphological aspects, two types of classic neovascularization are distinguished:

1. *Medusa-shaped lesion*, defined as a compact zone of small new blood vessels with minimal hypodense structure inside; the lesions are typically connected to a thicker main branch, which seem continuous from the outer retina into the more profound choroidal layers.
2. *Glomerulus-shaped lesion*, defined per comparison with the kidney glomerulus, harboring globular structures of entwined vessels that are separated by hypodense spaces.

Generally, the neovascular complex is surrounded by a dark zone located at choriocapillaris level, defined *"dark halo."* This aspect would correspond to a phenomenon of "vascular stealing" by the lesion against the surrounding choroid (Fig. 2.5).

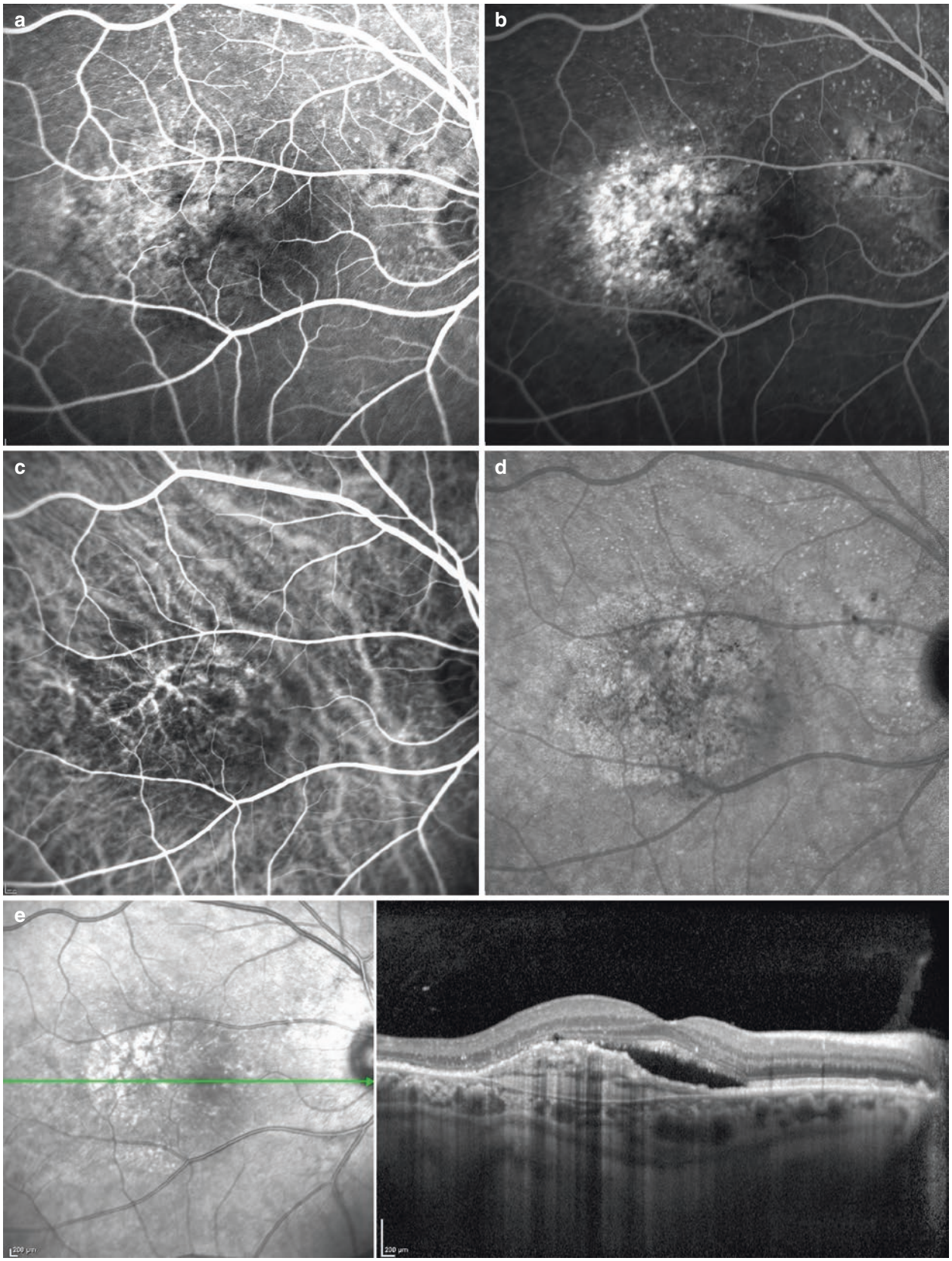

Fig. 2.3 Example of a patient with vascularized PED. (**a**) Fluorescein angiography reveals minimal stippled and irregular hyperfluorescence in the early phase and staining of the fibrovascular PED with the appearance of the characteristic pin-points in the later phases (**b**), consisting of an occult choroidal neovascular membrane; (**c**) indocyanine green angiography demonstrates a clear delineation of the neovascular complex in the early phase, revealing a well-defined area of hyperfluorescence, referred to as a "plaque," in the late phase (**d**); (**e**) SD-OCT shows an elevation of the RPE with sub-RPE heterogeneous signals consistent with a vascularized PED

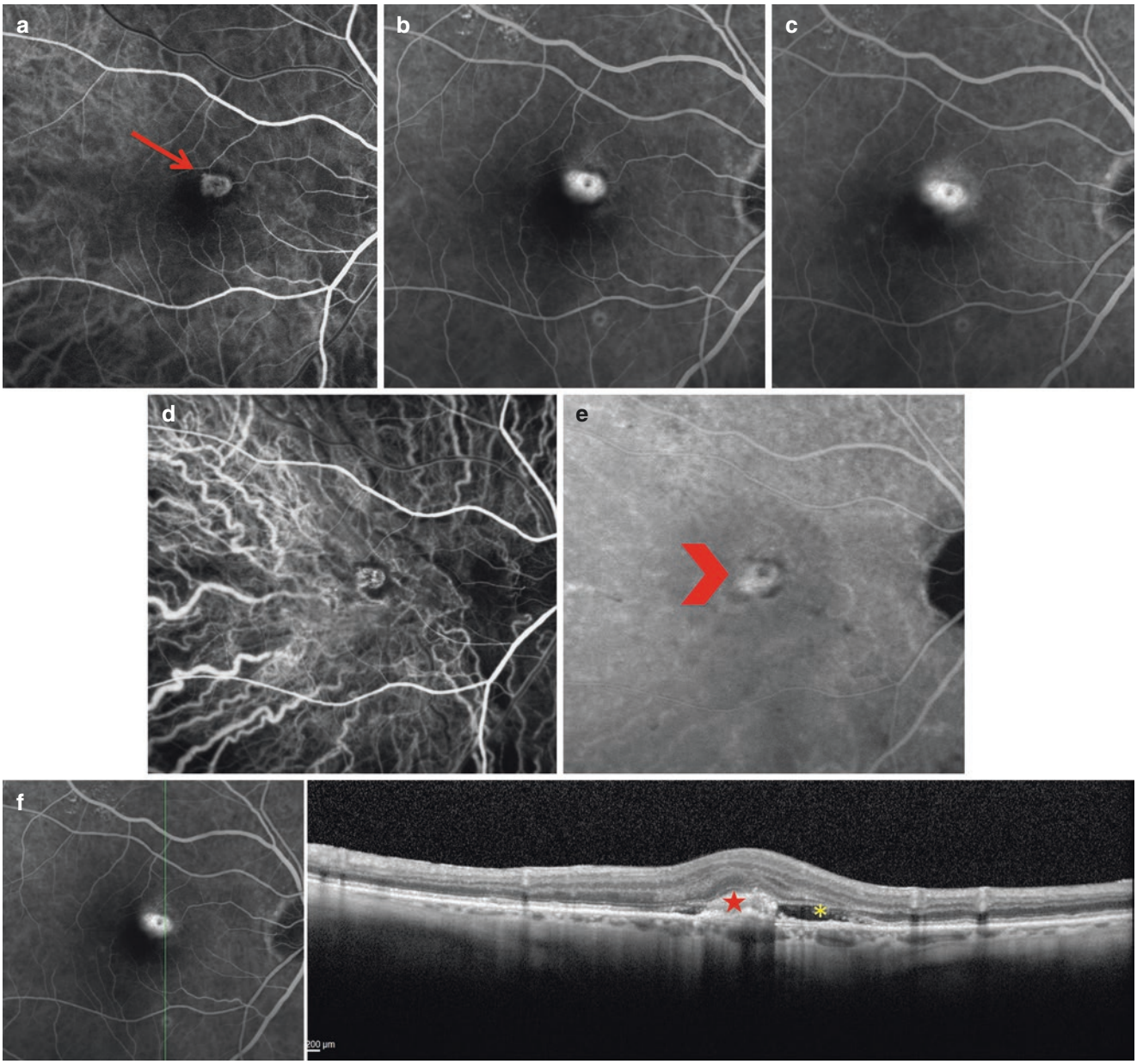

Fig. 2.4 Multimodal imaging of a patient with type 2 CNV in an exudative AMD patient. Fluorescein angiography shows, in early stages (**a**), the rapid filling of the neovascular membrane (arrow) which increases in intermediate stages (**b**) with leakage in late stages (**c**); indocyanine green angiography shows the filling of the neovascular membrane in early phases (**d**), with slight diffusion in late phases (arrow head) (**e**); (**f**) SD-OCT reveals the presence of a neovascular lesion, localized above the RPE (star), accompanied by serous detachment of neuroepithelium (asterisk) and subretinal exudation. Note the absence of drusen in this peculiar case

Mixed-Type Neovascularization

Most choroidal neovascularization secondary to AMD consists of a combination of type 1 and type 2 neovascularizations, also called predominantly "occult" or "classic" neovascularizations. If most new vessels are of type 1, lesion is defined as predominantly type 1 neovascularization or "minimally classic"; if, on the contrary, the lesion is predominantly of type 2, it is defined as "predominantly classic."

Type 3 Neovascularization

The term "type 3 Neovascularization" was introduced by Freund in 2008 (Freund et al. 2008).

The origin of type 3 neovascularization remains debated as to whether it arises from the retinal circulation or the choroidal circulation. Several anatomical findings correspond-

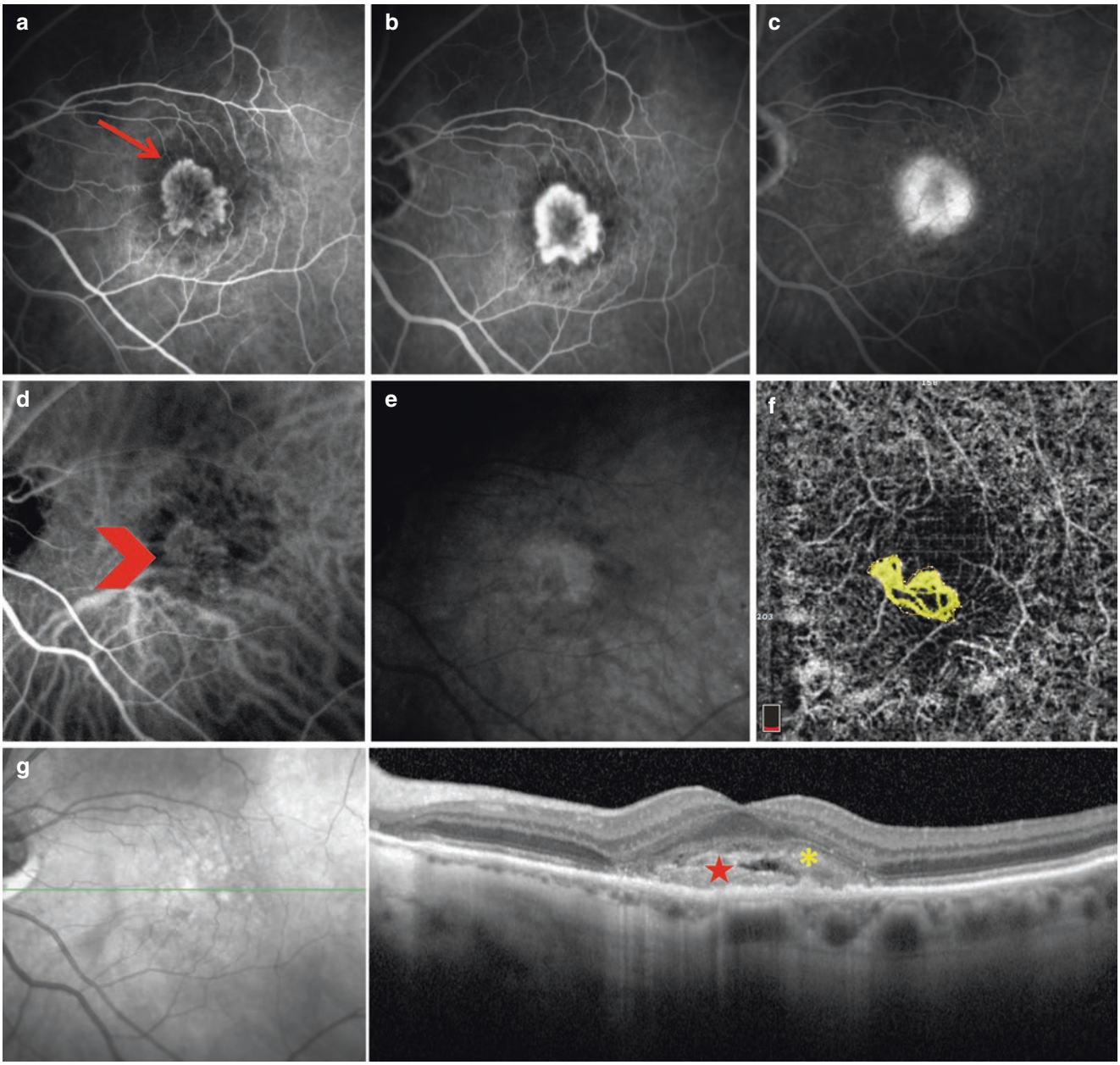

Fig. 2.5 Multimodal imaging of a patient with type 2 CNV. Fluorescein angiography shows, in early stages (**a**), the rapid filling of the neovascular membrane (arrow) which increases in intermediate stages (**b**) with leakage in late stages (**c**); indocyanine green angiography shows the filling of the neovascular membrane in early phases (arrow head) (**d**), with slight diffusion in late phases (**e**); (**f**) OCTA 3 × 3 (OptoVue) shows a high flow neovascular membrane in choriocapillaris segmentation; (**g**) SD-OCT shows the preepithelial neovascular lesion (star), accompanied by subretinal exudation (yellow asterisk) and a serous detachment of neuroepithelium

ing to type 3 NV have been described in the past: Hartnett, in 1992, defined the type 3 as "Abnormal deep retinal vascular complexes"; Kuhn, in 1995, described the "Chorio-Retinal Anastomosis" (CRA); Yannuzzi, in 2001, coined the term "Retinal Angiomatous Proliferation" (RAP); and Gass, in 2003, defined the "Occult choroidal retinal anastomosis" (OCRA).

Yannuzzi proposed three variants in the vasogenic process (Yannuzzi et al. 2008):

1. Initial focal retinal proliferation and progression
2. Initial focal choroidal proliferation and progression
3. Focal retinal proliferation with preexisting or simultaneous choroidal proliferation

More recent papers defined type 3 neovascularization as intraretinal neovascularization (Freund et al. 2008).

Drusenoid PED, intraretinal pigment migration, and focal outer retinal atrophy usually precede the development of type 3 NV. It has been demonstrated that drusenoid PED and focal photoreceptor and RPE loss precede type 3 neovascularization at the future site of lesion development, generating outer retinal atrophy, and ultimately allowing the deep capillary plexus to approach the RPE/sub-RPE space. The result of the increased vascular endothelial growth factor at this level may explain why sometimes type 3 neovascularization develops in close contact with the RPE/sub-RPE content (Querques et al. 2013a, b, c). Interestingly, it was recently demonstrated that although in the presence of a drusenoid PED, the exaggerated distance between the choroid and the photoreceptors drives this hypoxic response (Nagiel et al. 2015). In the absence of a PED, localized vascular endothelial growth factor production may arise from choroidal hypoperfusion.

In contrast to type 1 or type 2 NV, type 3 NV is commonly associated with intraretinal edema and is rarely associated with subretinal fluid.

On fundus examination, a small, deep, juxta-foveal intraretinal hemorrhage typically appears. The CRA is manifested by the sudden interruption of a retinal vessel whose diameter improves at 90° toward the choroid. Type 3 NVs are typically associated with the presence of reticular pseudodrusen at the posterior pole (Cohen et al. 2007b; Zweifel et al. 2010).

Fluorescein angiography usually reveals a hyperfluorescent hot-spot, localized at the termination of a retinal capillary branch. The lesion is frequently associated with an adjacent small hypofluorescence due to the masking effect of a punctuate hemorrhage. On late phases of the FA, the lesion is barely visible compared to the persisting hyperfluorescence corresponding to the "hot-spot," frequently accompanied by a cystoid macular edema in advanced type 3. ICGA shows the appearance of the feeder vessel in early stages appearing as a hyperfluorescent hot-spot that becomes more visible in late phases. The type 3 NV can sometimes be associated with a plaque on late phases, signaling the co-existence of a type 1 lesion. SD-OCT generally shows the intraretinal neovascular network, accompanied by cystoid edema and minimal subretinal fluid (Fig. 2.6).

An SD-OCT classification describing the evolution of type 3 NV in 3 phases has been proposed (Querques et al. 2010, 2013b, 2015):

- Phase 1 or *erosion sign*: appearance of early neovascularization from the choroid (characterized by a point of focal hyperfluorescence in angiography) which erodes the basement membrane of the RPE without breaking it.
- Phase 2 or *flap sign*: neovascularization infiltrates the outer layers of the retina forming an early type 3 (characterized by angiography by a hot-spot without serosanguinous PED).
- Phase 3 or *kissing sign*: infiltration of neovascularization in the inner layers of the retina and formation of a complete type 3 (characterized in angiography by a hot-spot associated with a serosanguinous PED).

Moreover, the choroidal thickness is typically more reduced in type 3 NV compared to type 1 and 2 CNV (Kim et al. 2013).

The early detection and treatment of type 3 NV is crucial not only because of the potential for rapid vision loss but also for a major regression of neovascular lesions following early anti-VEGF (Vascular Endothelial Growth Factor) therapy.

These neovascular lesions present a high rate of fellow eye involvement (about 100% by 3 years) (Gross et al. 2005).

Type 3 neovascularization, as described by Miere et al. (2015a, b), is characterized on OCTA by the presence of a retinal-retinal anastomosis emerging from the deep capillary plexus that forms a high-flow vascular network, called a "tuft," at the outer retina level, projecting at the sub-RPE space. Typically, at choriocapillaris segmentation, type 3 NV appears as a small high-flow lesion, defined *"clew-like,"* variously associated with the underlying choroidal vascularization by small interconnecting vessels (Fig. 2.7).

Polypoidal Choroidal Vasculopathy

Yannuzzi firstly described (Yannuzzi 1982) polypoidal choroidal vasculopathy (PCV) as an acquired, abnormal choroidal vasculopathy, distinct from typical CNV (Yannuzzi et al. 1990; Laude et al. 2010).

Originally described as a distinct entity occurring predominantly in African-American and Asian individuals between 50 and 65 years of age, PCV is actually considered as a form of type 1 neovascularization because the polyps appear to originate from neovascular tissue above the Bruch's membrane and is frequently associated with a branching vascular network. PCV is associated with choroidal abnormalities such as increased thickness, hyperpermeability, and pachyvessels.

PCV is characterized by single or multiple polypoidal vascular dilatations, accompanied by a type 1 CNV, and a "choroidal branching vascular network" (BVN), as observed on indocyanine green angiography (Yannuzzi et al. 1990; Laude et al. 2010; Yannuzzi 1982; Ciardella et al. 2004; Spaide et al. 1995).

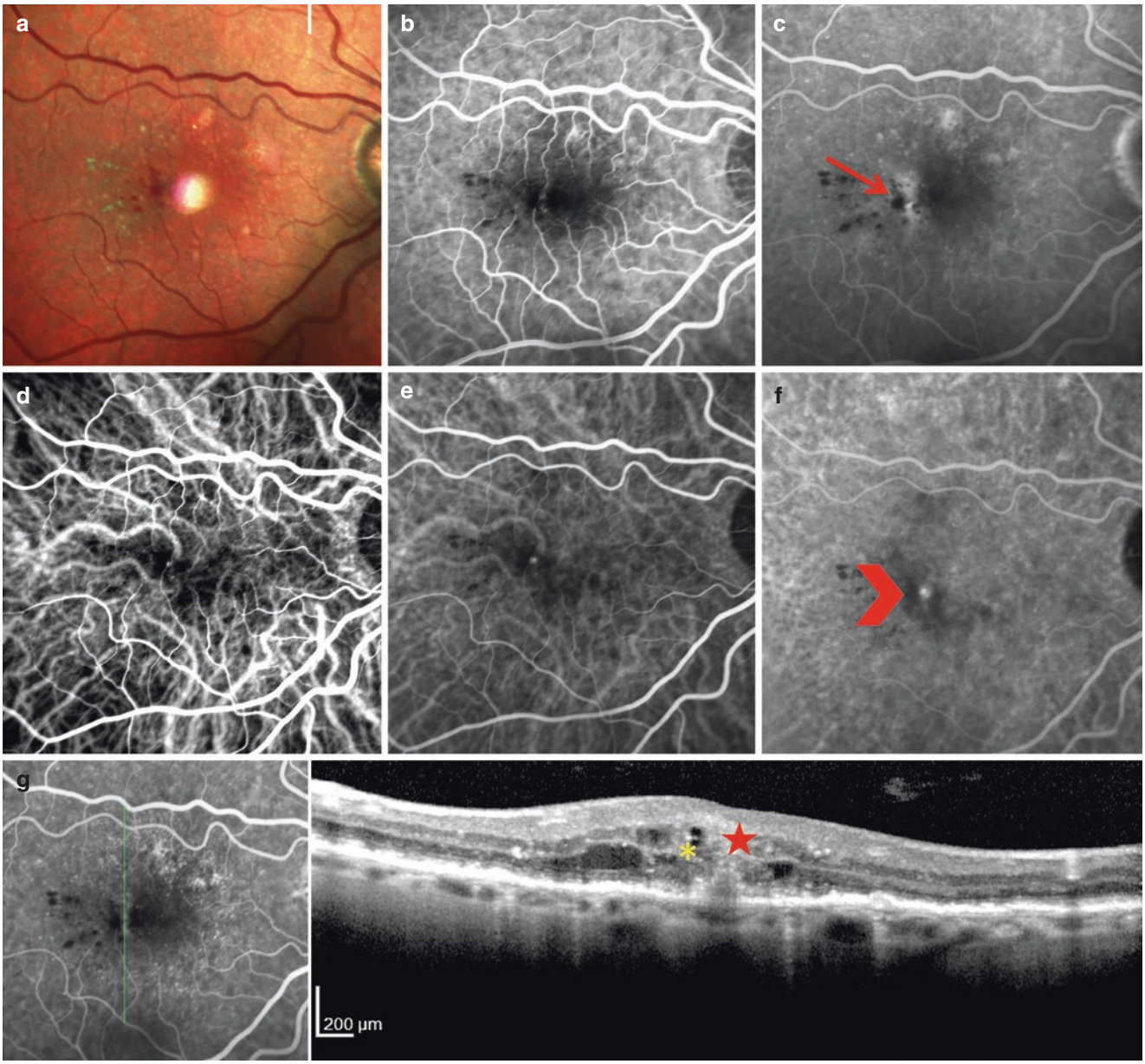

Fig. 2.6 Multimodal imaging of a patient with type 3 neovascularization: (**a**) Multicolor imaging shows the presence of small retinal hemorrhages at the fovea, accompanied by hard exudates, and reticular pseudodrusen wounds to the posterior pole; fluorescein angiography shows early hyperfluorescence (**b**), with late diffusion (arrow) (**c**); ICGA shows the appearance of the feeder vessel in early stages (**d**) and the typical "hot-spot" (arrowhead) persisting in late phases (**e**, **f**); (**g**) SD-OCT shows the "kissing sign" (star), accompanied by cystoid edema (asterisk) and small, hyper-reflective spots

On SD-OCT, the polypoidal dilations appear as dome-like elevations of RPE with moderate internal reflectivity (Sa et al. 2005; Iijima et al. 1999; Otsuji et al. 2000; De Salvo et al. 2014).

The branching neovascular network presents as two highly reflective lines ("double layer sign") (Sato et al. 2007).

Srour et al. (2016) recently showed the OCTA features of PCV. The authors demonstrated that OCTA could visualize different structures in PCV. On the choriocapillaris segmentation, OCTA constantly showed the BVN, appearing as a hyperflow lesion, and polypoidal lesions, appearing either as a hyperflow round structure surrounded by a hypointense halo, or as a hypoflow round structure (Fig. 2.8).

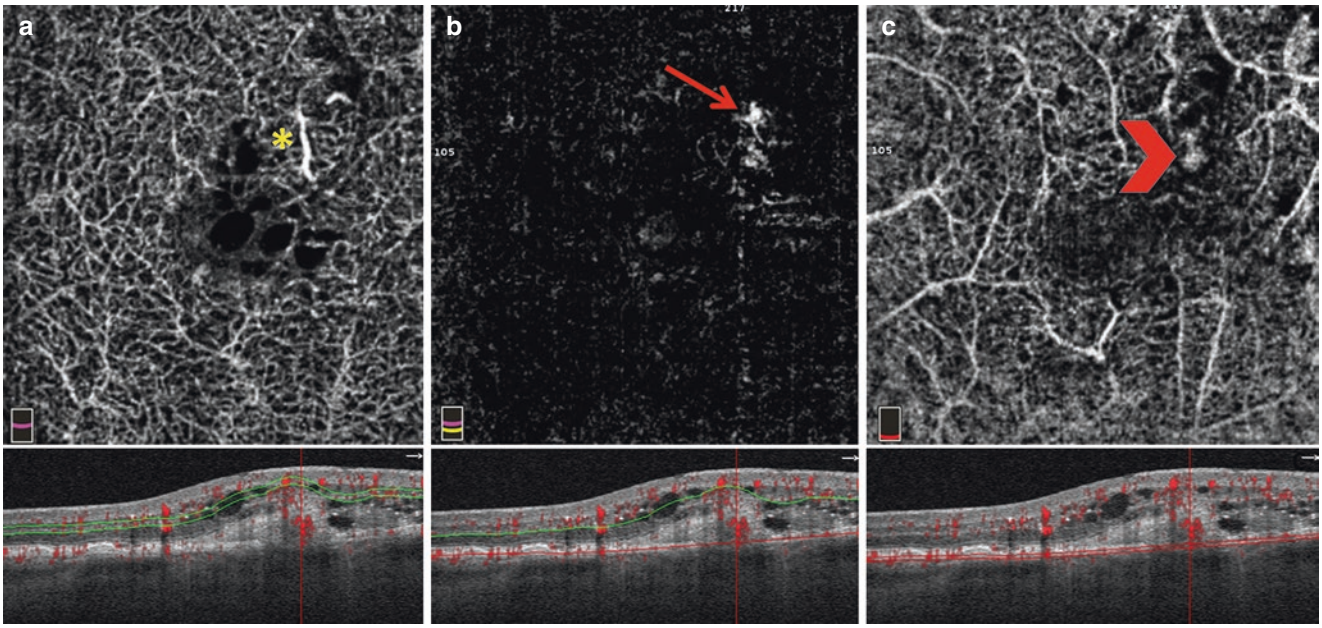

Fig. 2.7 OCTA of a patient with type 3 neovascularization. 3 × 3 OCTA scans (OptoVue) with correspondent B-scans. (**a**) The deep capillary plexus segmentation shows a small, high-flow vessel that deepens in the external retinal layers (asterisk); (**b**) high-flow "tuft-shaped" lesion (arrow) at outer retina segmentation; (**c**) choriocapillaris segmentation shows the presence of the characteristic "clew-like lesion" (arrow head) apparently connected with the "tuft"

In most cases the polypoidal lesions appeared as hypoflow round structures; this absence of signal does not mean that there is no blood flow, but rather that blood flow is not within the level of detection of the OCTA device.

The non-visualization of the vascular structure may be due to an increased (turbulent flow) or decreased flow within the polyps.

Subretinal Fibrosis

Neovascular lesions resemble a dynamic wound healing process characterized by inflammation, angiogenesis, and fibrosis (Schlingemann 2004).

The subretinal fibrosis is the result of neovascular tissue remodeling, a sign of advanced neovascular lesions, repeated bleeding, macrophagic invasion, and healing.

Several studies have shown the risk of evolution toward macular atrophy and/or subretinal fibrosis of the treated CNV (Bloch et al. 2013; Channa et al. 2015; Toth et al. 2015; Rosenfeld et al. 2011; Cohen et al. 2012).

Nevertheless, subretinal fibrosis may also occur as the consequence of repeated subfoveal hemorrhages (Hwang et al. 2011).

On fundus examination, subretinal fibrosis appears as a well-demarcated, elevated mound of yellowish-white tissue (Fig. 2.9).

Multicolor imaging may help in the diagnosis showing a white/green dome-shaped elevation at the posterior pole.

Fluorescein angiography generally reveals early and intense staining of the dye in late phases of the sequence. SD-OCT shows subretinal hyperreflective lesions, of variable size and location, with possible loss of adjacent retinal pigment epithelium and ellipsoid zone. In the absence of associated exudative component, no leakage is visible.

As showed by Miere et al. (2015b) the OCTA allowed the visualization and analysis of subretinal fibrosis (Fig. 2.10).

A complete lack of signal, possibly blocked by the fibrous scar, generating a complete masking effect of the lesion, was the only discernible feature on OCTA images for 3 out of 49 patients (6.2% of the whole study population).

The authors described three different neovascularization phenotypes inside the fibroglial scar: pruned vascular tree pattern (53.1%), tangled network pattern (28.6%), and/or vascular loop (51.0%). Two features, "large flow void" and a "dark halo," have been associated with subretinal fibrosis, presenting as an obscure zone surrounding the neovascular network. Pruned vascular tree pattern was characterized by an irregular, filamentous flow inside the neovascular network on the OCTA scans, comprising only important vessels, with thinner capillaries not visible. In all cases of pruned vascular tree, a large central feeder vessel was detected. Tangled network was characterized by an abnormal, high flow,

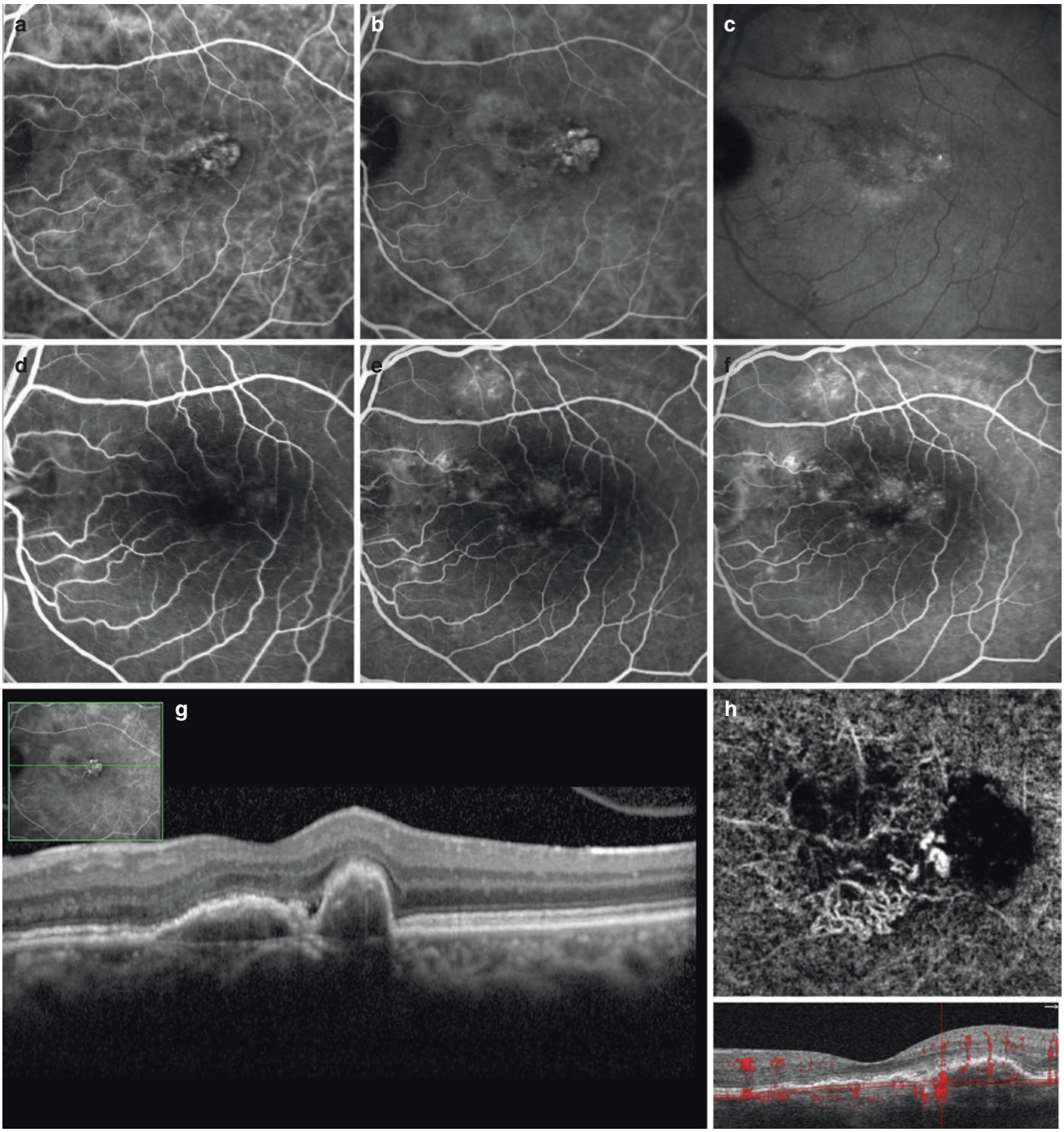

Fig. 2.8 Multimodal imaging of a patient with polypoidal choroidal vasculopathy: (**a**) ICGA shows the early filling of polypoidal lesions and the BVN, persisting in the intermediate phases (**b**) and the wash-out in late phases (**c**); fluorescein angiography shows an inhomogeneous hyperfluorescence during all the angiographic sequence (**d**–**f**); SD-OCT shows the polypoidal lesions accompanied by the BVN (**g**); OCTA 3 × 3 scan shows two different high-flow lesions, corresponding to the polyps, and a hypodense lesion corresponding to the PED and the high-flow BVN (**h**)

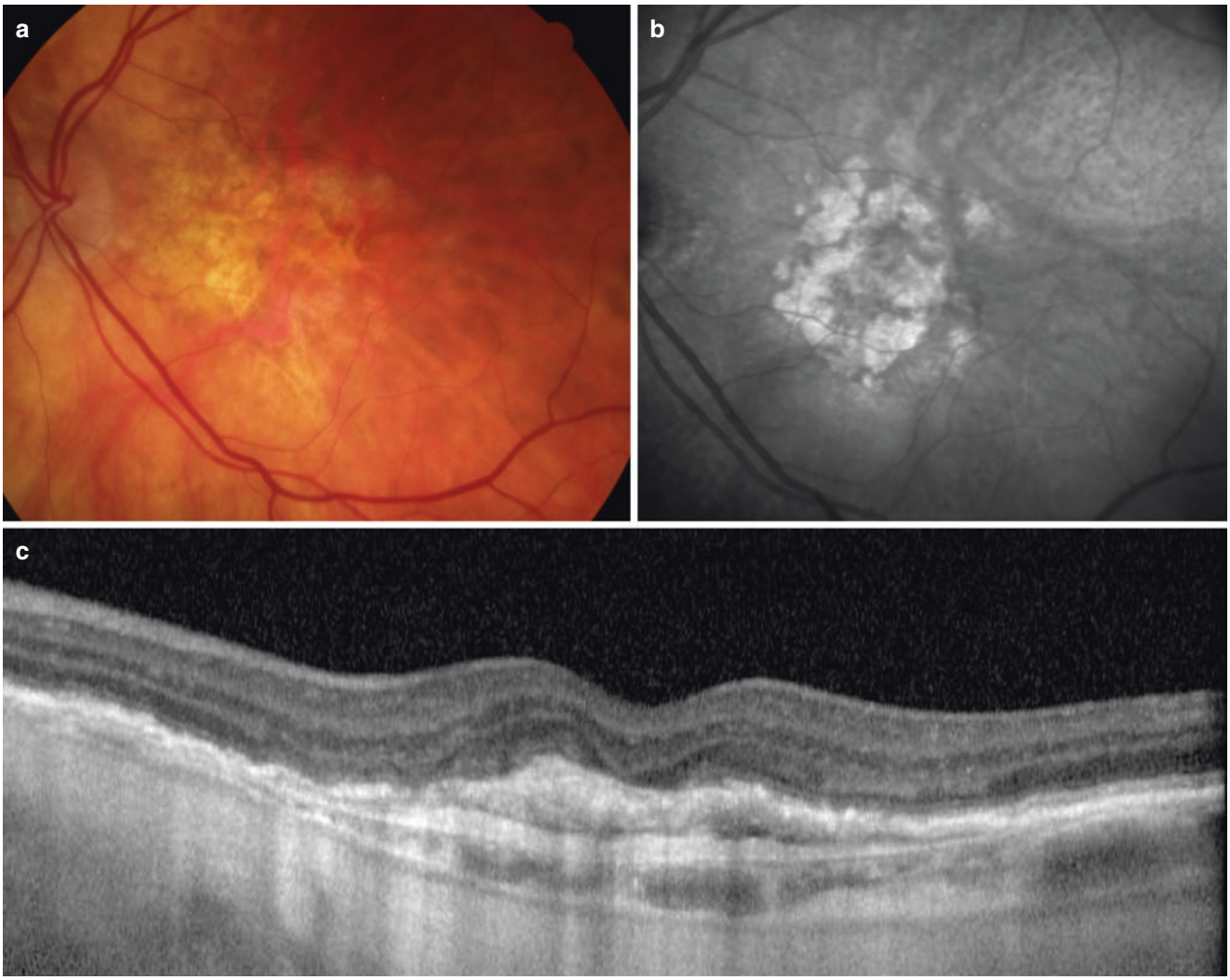

Fig. 2.9 Multimodal imaging of a patient with subretinal fibrosis. (**a**) Color fundus photo showing well-demarcated, elevated mound of yellowish-white tissue; (**b**) Infrared imaging reveals a greyish-white aspect of subretinal fibrosis; (**c**) SD-OCT shows the homogeneous hyperreflective lesion located in subretinal space

frequently interlacing vascular network in the automatic segmentation zone corresponding to the fibrotic scar on the B-scan image. Vascular loop was defined as a high flow with a convoluted network on the OCTA scans.

Management: Anti-VEGF Therapy

The anti-VEGFs have become the gold standard for the treatment of neovascular AMD. Laser photocoagulation and photodynamic therapy (PDT) are no longer the first-line treatments of CNV complicating AMD. VEGF is secreted by RPE cells, causing endothelial cell proliferation and vascular permeability increase. VEGF has a pivotal role in neovascular AMD. The cascade of VEGF-induced angiogenesis could be stopped at different stages; this fact has led to the development of several VEGF targeting molecules.

There are four therapeutic molecules targeting the VEGF for the treatment of neovascular AMD.

The Anti-VEGFs

Pegaptanib (Macugen®)

Pegagtanib was the first molecule that showed an effectiveness in neovascular AMD. Its effectiveness was partial by showing less loss of visual acuity compared to the control group. Its use has decreased considerably since the availability of the new anti-VEGFs.

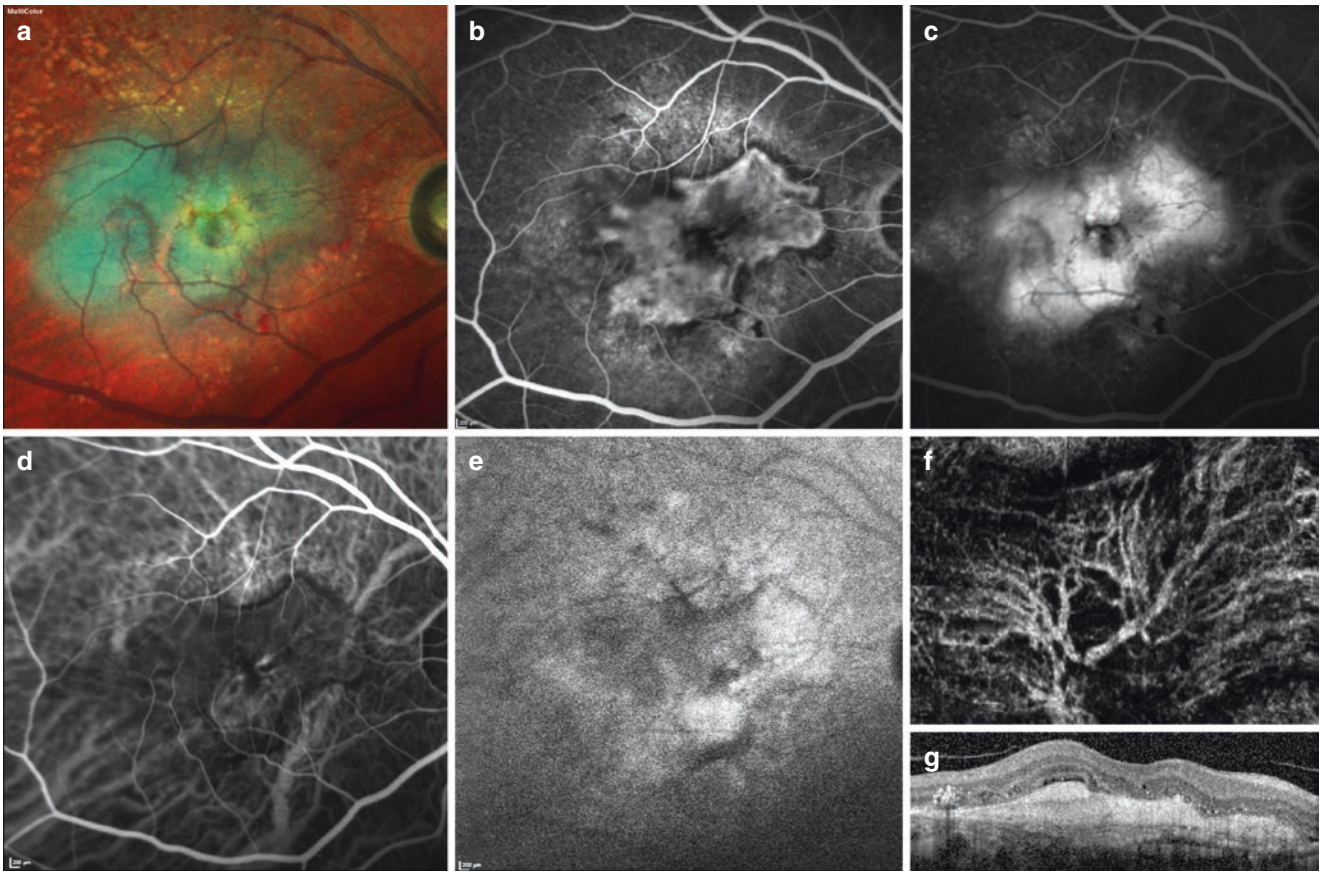

Fig. 2.10 Multimodal imaging of a patient with subretinal fibrosis. (**a**) Multicolor imaging shows a yellowish-green elevated lesion, involving the macula and extending at the posterior pole. Fluorescein angiography reveals the staining of the lesion (**b**) with no leakage in late stages (**c**); ICGA shows rapid filling of neovascular network (**d**) and late hyperfluorescence (**e**). Note the hypofluorescent borders of the lesion, corresponding to the neovascular tissue retraction, during all the angiographic sequence; (**f**) OCTA scan in the outer retina segmentation reveals the large central feeder vessel, few emergent collateral branches, along with the absence of flow between the large branches; (**g**) SD-OCT showing subretinal hyperreflective lesion with loss of adjacent retinal pigment epithelium and ellipsoid zone

Bevacizumab (Avastin®) and Ranibizumab (Lucentis®)

Bevacizumab is a full-length humanized monoclonal antibody directed against VEGF-A.

Ranibizumab is an Fab fragment of an anti-VEGF humanized monoclonal antibody.

This low molecular weight molecule consists of a non-binding sequence of human origin (decreasing the antigenicity of this molecule) and contains a high-affinity sequence for VEGF-A.

The efficacy of bevacizumab has been demonstrated in several large studies (CATT and GEFAL) (CATT Research Group et al. 2011; Kodjikian et al. 2013).

The effectiveness of ranibizumab in monthly injections has been clearly demonstrated in several randomized controlled trials. The pivotal studies that led to its use were MARINA (gain of 6.6 letters ETDRS at 24 months) (Rosenfeld et al. 2006) and ANCHOR (gain of 11.3 letters at 1 year, a difference of 20.8 letters compared to the group PDT) (Brown et al. 2009).

Regarding the use of the two molecules (ranibizumab and bevacizumab), the studies show no significant difference in efficacy between the two treatments (CATT, GEFAL, IVAN) (CATT Research Group et al. 2011; Kodjikian et al. 2013; IVAN Study Investigators et al. 2012).

Aflibercept (Eylea®)

Aflibercept is a recombinant fusion protein: VEGF-Trap. The evaluation of its efficacy in the treatment of exudative AMD is based on the two pivotal studies VIEW1 and VIEW2 of non-inferiority compared to ranibizumab (Heier et al. 2012). The results showed similar efficacy and safety between the two molecules at 52 and 96 weeks (7.9 letters gain in the ranibizumab monthly group and 7.6 letters in the aflibercept group).

Therapeutic Protocols

Fixed Protocols

Fixed protocols are the first therapeutic protocols proposed in anti-VEGF, with strict monthly protocols (Rosenfeld et al. 2006) where patients routinely receive a monthly injection, regardless of the neovascular activity.

The PIER study attempted to reduce the rate of routine injections to quarterly injections (fixed regimen of three IVT ranibizumab followed by quarterly injections), but it scored lower than the previous two pivotals (Regillo et al. 2008).

The strict bi-monthly protocol ("Q8") consists of a systematic administration every 2 months, after the first phase of 3 monthly injections.

This type of protocol has the advantage of regularity and continuous intra-vitreous antiangiogenic coverage.

However, the fixed and repeated nature of these so-called "proactive" protocols may place many patients in the potential position of treatment, with a theoretical increase in the risk of endophthalmitis.

Indeed, several studies have shown that a proportion of patients did not require a new injection after the induction phase in the first year (20% in the SUSTAIN study) (Holz et al. 2011). Finally, repeated injections of anti-VEGF may induce a potential risk for chorioretinal atrophy.

Protocols on Demand

The PrONTO study evaluated patients' therapeutic retreatment strategy (ranibizumab) based on the results of monthly clinical examination and OCT data, following an induction phase of 3 monthly intravitreal injections.

This protocol appears to be as effective as a functionally stable monthly regimen with a lower IVT number (Lalwani et al. 2009) finding a visual acuity gain of 9.3 letters at 1 year, with 5.6 injections (versus 12 in MARINA and ANCHOR studies).

This is a "Pro-Re-Nata" (PRN) treatment regimen that was quickly adopted. Subsequently, other studies have confirmed the equivalence of this protocol to fixed monthly schedules in terms of visual gain. There are some adjustments to this PRN protocol: when it includes a series of successive systematic injections, it is called reinforced PRN, and when an injection is programmed systematically at regular intervals, whatever the exudative activity, the PRN is called "cappé."

Evolutionary Protocols

A third strategy has been proposed: the "Treat and Extend" which aims to reduce the number of visits while maintaining the gain in visual acuity.

It consists of reviewing the patients after the induction phase of three IVT (Spaide 2007): in case of persistence of the exudation, the patients are treated and reviewed again at 4 weeks. In case of absence of exudation, they will still be treated ("Treat") but the time of the next control will be extended ("Extend"). Monitoring can therefore be progressively spaced.

Thus, schematically, the patient will be treated at each visit and the interval is gradually increased by 2 weeks in the absence of exudation up to a maximum of 12 weeks. On the other hand, in the presence of exudation, the interval is reduced by 2 weeks to a minimum of 4 weeks. This approach has the advantage of a gradual individualization of the treatment but also presents obvious risks of over or under treatment.

Recently, a new protocol has been described: the "Observe and Plan" protocol (Mantel et al. 2014). It is based on the principle that the exudative reactivation delay after the induction phase will condition future recurrence intervals.

Thus, patients will receive a series of three systematic IVT followed by a monthly observation period "Observe" which will determine the interval between the third injection and the appearance of exudative signs on OCT, and this interval will be decreased by 2 weeks.

From here, a fixed individual treatment "Plan" of three new injections whose achievement interval was set during the observation period is realized.

Then, at the end of this new series of IVT if neovascular activity persists, the interval is further reduced by 2 weeks for the following three systematic IVT, otherwise, the interval is increased by 2 weeks and so after.

This protocol reduces the number of total visits over the year but also presents a risk for over-treatment.

There is currently no consensus on the strategy to follow when monitoring patients. It is important to individualize the therapeutic protocol according to the profile of recurrence of the patient after an observation phase.

References

Bloch SB, Lund-Andersen H, Sander B, Larsen M. Subfoveal fibrosis in eyes with neovascular age-related macular degeneration treated with intravitreal ranibizumab. Am J Ophthalmol. 2013;156:116–24.

Brown DM, Michels M, Kaiser PK, et al. Ranibizumab versus verteporfin photodynamic therapy for neovascular age-related macular degeneration: two-year results of the ANCHOR study. Ophthalmology. 2009;116:57–65.e5.

CATT Research Group, Martin DF, Maguire MG, Ying G, et al. Ranibizumab and bevacizumab for neovascular age-related macular degeneration. N Engl J Med. 2011;364:1897–908.

Channa R, Sophie R, Bagheri S, et al. Regression of choroidal neovascularization results in macular atrophy in anti-vascular endothelial growth factor-treated eyes. Am J Ophthalmol. 2015;159:9–19.

Ciardella AP, Donsoff IM, Huang SJ, et al. Polypoidal choroidal vasculopathy. Surv Ophthalmol. 2004;49:25–37.

Cohen SY, Creuzot-Garcher C, Darmon J, et al. Types of choroidal neovascularization in newly diagnosed exudative age-related macular degeneration. Br J Ophthalmol. 2007a;91:1173–6.

Cohen SY, Dubois L, Tadayoni R, et al. Prevalence of reticular pseudodrusen in age-related macular degeneration with newly diagnosed choroidal neovascularisation. Br J Ophthalmol. 2007b;91:354–9.

Cohen SY, Oubraham H, Uzzan J, et al. Causes of unsuccessful ranibizumab treatment in exudative age-related macular degeneration in clinical settings. Retina. 2012;32:1480–5.

Coscas G, De Benedetto U, Coscas F, et al. Hyperreflective dots: a new spectral-domain optical coherence tomography entity for follow-up and prognosis in exudative age-related macular degeneration. Int J Ophthalmol. 2013;229:32–7.

De Salvo G, Vaz-Pereira S, Keane PA, et al. Sensitivity and specificity of spectral-domain optical coherence tomography in detecting idiopathic polypoidal choroidal vasculopathy. Am J Ophthalmol. 2014;158:1228–38.e1.

El Ameen A, Cohen SY, Semoun O, et al. Type 2 neovascularization secondary to age-related macular degeneration imaged by optical coherence tomography angiography. Retina. 2015;35:2212–8.

Ferris FL III, Fine SL, Hyman L. Age related macular degeneration and blindness due to neovascular maculopathy. Arch Ophthalmol. 1984;102:1640–2.

Freund B, Ho I-V, Barbazetto I, et al. Type 3 neovascularization. The expanded spectrum of retinal angiomatous proliferation. Retina. 2008;28:201–11.

Freund KB, Zweifel SA, Engelbert M. Do we need a new classification for choroidal neovascularization in age-related macular degeneration? Retina. 2010;30:1333–49.

Gass JDM, Agarwal A, Lavina AM, et al. Focal inner retinal hemorrhages in patients with drusen: an early sign of occult choroidal anastomosis. Retina. 2003;23:241–51.

Gelisken F, Inhoffen W, Schneider U, et al. Indocyanine green angiography in classic choroidal neovascularization. Jpn J Ophthalmol. 1998;42:300–3.

Gross NE, Aizman A, Brucker A, Klancnik JM Jr, Yannuzzi LA. Nature and risk of neovascularization in the fellow eye of patients with unilateral retinal angiomatous proliferation. Retina. 2005;25:713–8.

Grossniklaus HE, Gass JD. Clinicopathologic correlations of surgically excised type 1 and type 2 submacular choroidal neovascular membranes. Am J Ophthalmol. 1998;126:59–69.

Hartnett ME, Weiter JJ, Gardts A, Jalkh AE. Classification of retinal pigment epithelial detachments associated with drusen. Graefes Arch Clin Exp Ophthalmol. 1992;230:11–9.

Heier JS, Brown DM, Chong V, et al. Intravitreal aflibercept (VEGF trap-eye) in wet age-related macular degeneration. Ophthalmology. 2012;119:2537–48.

Holz FG, Amoaku W, Donate J, et al. Safety and efficacy of a flexible dosing regimen of ranibizumab in neovascular age-related macular degeneration: the SUSTAIN study. Ophthalmology. 2011;118:663–71.

Hwang JC, Del Priore LV, Freund KB, et al. Development of subretinal fibrosis after anti-VEGF treatment in neovascular age-related macular degeneration. Ophthalmic Surg Lasers Imaging. 2011;42:6–11.

Iijima H, Imai M, Gohdo T, et al. Optical coherence tomography of idiopathic polypoidal choroidal vasculopathy. Am J Ophthalmol. 1999;127:301–5.

IVAN Study Investigators, Chakravarthy U, Harding SP, Rogers CA, et al. Ranibizumab versus bevacizumab to treat neovascular age-related macular degeneration: one-year findings from the IVAN randomized trial. Ophthalmology. 2012;119:1399–411.

Jung JJ, Chen CY, Mrejen S, et al. The incidence of neovascular subtypes in newly diagnosed neovascular age-related macular degeneration. Am J Ophthalmol. 2014;158:769–79.

Kim JH, Kim JR, Kang SJ, Ha HS. Thinner choroid and greater drusen extent in retinal angiomatous proliferation than in typical exudative age-related macular degeneration. Am J Ophthalmol. 2013;155(743–9):749.

Kodjikian L, Souied EH, Mimoun G, et al. Ranibizumab versus bevacizumab for neovascular age-related macular degeneration: results from the GEFAL noninferiority randomized trial. Ophthalmology. 2013;120:2300–9.

Kuehlewein L, Bansal M, Lenis LT, et al. Optical coherence tomography angiography of type 1 neovascularization in age-related macular degeneration. Am J Ophthalmol. 2015;160:739–48.

Kuhn D, Meunier I, Soubrane G, Coscas G. Imaging of chorioretinal anastomoses in vascularized retinal pigment epithelium detachments. Arch Ophthalmol. 1995;113:1392–8.

Lalwani GA, Rosenfeld PJ, Fung AE, et al. A variable-dosing regimen with intravitreal ranibizumab for neovascular age-related macular degeneration: year 2 of the PrONTO Study. Am J Ophthalmol. 2009;148:43–58.e1.

Lam D, Semoun O, Blanco-Garavito R, et al. Wrinkled vascularized retinal pigment epithelium detachment prognosis after intravitreal anti-VEGF therapy. Retina. 2017;38:1100–9.

Laude A, Cackett PD, Vithana EN, et al. Polypoidal choroidal vasculopathy and neovascular age-related macular degeneration: same or different disease? Prog Retin Eye Res. 2010;29:19–29.

Mantel I, Niderprim S-A, Gianniou C, et al. Reducing the clinical burden of ranibizumab treatment for neovascular age-related macular degeneration using an individually planned regimen. Br J Ophthalmol. 2014;98:1192–6.

Miere A, Querques G, Semoun O, et al. Optical coherence tomography angiography in early type 3 neovascularization. Retina. 2015a;35:2236–41.

Miere A, Semoun O, Cohen SY, et al. Optical coherence tomography angiography features of subretinal fibrosis in age-related macular degeneration. Retina. 2015b;35:2275–84.

Mrejen S, Sarraf D, Mukkamala SK, Freund KB. Multimodal imaging of pigment epithelial detachment: a guide to evaluation. Retina. 2013;33:1735–62.

Nagiel A, Sarraf D, Sadda SR, et al. Type 3 neovascularization: evolution, association with pigment epithelial detachment, and treatment response as revealed by spectral domain optical coherence tomography. Retina. 2015;35:638–47.

Ores R, Puche N, Querques G, et al. Gray hyper-reflective subretinal exudative lesions in exudative age-related macular degeneration. Am J Ophthalmol. 2014;158:354–61.

Otsuji T, Takahashi K, Fukushima I, et al. Optical coherence tomographic findings of idiopathic polypoidal choroidal vasculopathy. Ophthalmic Surg Lasers. 2000;31:210–4.

Pang CE, Messinger JD, Zanzottera EC, et al. The Onion Sign in neovascular age-related macular degeneration represents cholesterol crystals. Ophthalmology. 2015;122:2316–26.

Querques G, Atmani K, Berboucha E, et al. Angiographic analysis of retinal-choroidal anastomosis by confocal scanning laser ophthalmoscopy technology and corresponding (eye-tracked) spectral-domain optical coherence tomography. Retina. 2010;30:222–34.

Querques G, Querques L, Forte R, et al. Precursors of type 3 neovascularization: a multimodal imaging analysis. Retina. 2013a;33:1241–8.

Querques G, Souied EH, Freund KB. Multimodal imaging of early stage 1 type 3 neovascularization with simultaneous eye-tracked spectral-domain optical coherence tomography and high-speed real-time angiography. Retina. 2013b;33:1881–7.

Querques G, Srour M, Massmaba N, et al. Functional characterization and multimodal imaging of treatment-naive "quiescent" choroidal neovascularization. Invest Ophthalmol Vis Sci. 2013c;54:6886–92.

Querques G, Souied EH, Freund KB. How has high-resolution multimodal imaging refined our understanding of the vasogenic process in type 3 neovascularization? Retina. 2015;35:603–13.

Querques G, Capuano V, Costanzo E, et al. Retinal pigment epithelium aperture: a previously unreported finding in the evolution of avascular pigment epithelium detachment. Retina. 2016;36(Suppl 1):S65–72.

Rahimy E, Freund KB, Larsen M. Multilayered pigment epithelial detachment in neovascular age-related macular degeneration. Retina. 2014;34:1289–95.

Regillo CD, Brown DM, Abraham P, et al. Randomized, double-masked, sham-controlled trial of ranibizumab for neovascular age-related macular degeneration: PIER Study year 1. Am J Ophthalmol. 2008;145:239–48.

Rosenfeld PJ, Brown DM, Heier JS, et al. Ranibizumab for neovascular age-related macular degeneration. N Engl J Med. 2006;355:1419–31.

Rosenfeld PJ, Shapiro H, Tuomi L, et al. Characteristics of patients losing vision after 2 years of monthly dosing in the phase III ranibizumab clinical trials. Ophthalmology. 2011;118:523–30.

Sa HS, Cho HY, Kang SW. Optical coherence tomography of idiopathic polypoidal choroidal vasculopathy. Korean J Ophthalmol. 2005;19:275–80.

Sato T, Kishi S, Watanabe G, et al. Tomographic features of branching vascular networks in polypoidal choroidal vasculopathy. Retina. 2007;27:589–94.

Schlingemann RO. Role of growth factors and the wound healing response in age-related macular degeneration. Graefes Arch Clin Exp Ophthalmol. 2004;242:91–101.

Semoun O, Guigui B, Tick S, et al. Infrared features of classic choroidal neovascularization in exudative age related macular degeneration. Br J Ophthalmol. 2009;93:182–5.

Spaide R. Ranibizumab according to need: a treatment for age-related macular degeneration. Am J Ophthalmol. 2007;143:679–80.

Spaide RF, Yannuzzi LA, Slakter JS, et al. Indocyanine green videoangiography of idiopathic polypoidal choroidal vasculopathy. Retina. 1995;15:100–10.

Srour M, Querques G, Semoun O, et al. Optical coherence tomography angiography characteristics of polypoidal choroidal vasculopathy. Br J Ophthalmol. 2016;100(11):1489–93.

Toth LA, Stevenson M, Chakravarthy U. Anti-vascular endothelial growth factor therapy for neovascular age-related macular: outcomes in eyes with poor initial vision. Retina. 2015;35:1957–63.

Yannuzzi LA. Idiopathic polypoidal choroidal vasculopathy. Presented at The Macula Society Meeting. Miami; 1982.

Yannuzzi LA, Sorenson J, Spaide RF, et al. Idiopathic polypoidal choroidal vasculopathy (IPCV). Retina. 1990;10:1–8.

Yannuzzi LA, Negrão S, Iida T, et al. Retinal angiomatous proliferation in age-related macular degeneration. Retina. 2001;21:416–34.

Yannuzzi LA, Freund KB, Takahashi BS. Review of retinal angiomatous proliferation or type 3 neovascularization. Retina. 2008;28:375–84.

Zweifel SA, Spaide RF, Curcio CA, Malek G, Imamura Y. Reticular pseudodrusen are subretinal drusenoid deposits. Ophthalmology. 2010;117:303–12.e1.